Drug Design, Development and Therapy

Dovepress
open access to scientific and medical research

Open Access Full Text Article

ORIGINAL RESEARCH

Recombinant Human Adenovirus Type 5 (H101) Intra-Tumor Therapy in Patients with Persistent, Recurrent, or Metastatic Cervical Cancer: Genomic Profiling Relating to Clinical Efficacy

Qiying Zhang[1], Jing Zhang[1], Zi Liu[1,2], Juan Wang[1], Fei Wang[1], Tao Wang[1], Fan Shi[1], Jin Su[1], Yalong Zhao[3]

[1]Department of Radiation Oncology, the First Affiliated Hospital of Xi'an Jiaotong University, Xi'an, 710061, People's Republic of China; [2]Biobank, the First Affiliated Hospital of Xi'an Jiaotong University, Xi'an, 710061, People's Republic of China; [3]Department of Medical Affairs, Guangdong Techpool Bio-Pharma Co, Ltd, Guangzhou, 510000, People's Republic of China

Correspondence: Zi Liu, Department of Radiation Oncology, the First Affiliated Hospital of Xi'an Jiaotong University, No. 277, West Yanta Road, Xi'an, Shaanxi, 710061, People's Republic of China, Tel +86-18991232167, Email liuzmail@126.com

Objective: Genomic profiles relating to H101 treatment-induced alterations are yet to be achieved. Here, we evaluated the impact of H101 via exome-sequencing approaches aiming to probe for potential biomarkers that are actionable in the treatment of persistent/recurrent/metastatic (P/R/M) cervical cancer.

Methods: Whole exome sequencing (WES) was performd on paired pre- and post-H101 samples from 17 P/R/M cervical cancer patients who received serial intra-tumor injections of H101. Somatic mutations, including high-frequency mutations, microsatellite instability (MSI) status, tumor mutation burden (TMB), clonal evolution, and mutational signature were analyzed.

Results: The median follow-up time after the H101 treatment was 14 months. Complete response was achieved in 9 patients, 3 patients achieved partial response, and 2 patients had stable disease, resulting in an objective response rate (ORR) of 70.6% (95% CI: 46.4%-96.7%). WES analysis showed no difference in treatment-related mutation characteristics, including non-synonymous-SNVs and TMB status. Patients with lower TMB were correlated with improved H101 response rates (P=0.044), whereas the same was not evident in high MSI (MSI-H) versus non-MSI-H patients (P=0.528). We observed a few high-frequency mutation genes (TTN, KMT2D, ALDOA, DNAH7, ADAP1, PTPN23, and THEMIS2) that probably carry functional importance in response to H101 treatment, among which KMT2D and ADAP1 mutations were associated with inferior progression-free survival (PFS) and/or overall survival (OS) (P<0.05). Notably, H101 treatment-induced accumulating subclones or clusters in primary tumors and some (Signature 2) were associated with shorter PFS.

Conclusion: We conducted an unprecedented work via a WES-based approach and provided preliminary insights into H101 treatment-induced genetic aberrations in which some genes (TTN, KMT2D, ALDOA, DNAH7, ADAP1, PTPN23, and THEMIS2) could be considered potential therapeutic targets of H101-containing treatment in cervical carcinoma. Moreover, the therapy-associated characteristics such as clonal evolution and a mutational signature may warrant further evaluation of H101 in clinical settings for treating cervical carcinoma.

Keywords: cervical cancer, recombinant human adenovirus type 5, H101, whole exome sequencing, genomic profiling, therapeutic targets

Introduction

Patients with persistent, recurrent, or metastatic (P/R/M) cervical carcinoma respond poorly to treatment despite the best available therapeutic regimens, with a 5-year survival of 17%.[1] Most of them are heavily pretreated with chemotherapy and/or radiotherapy, and many patients experience complications related to treatment or advanced disease, which exclude

Received: 1 August 2023
Accepted: 7 November 2023
Published: 27 November 2023

them from clinical trial enrollment. Immunotherapy has desirable potency for certain virally associated epithelial malignancies such as cervical[2,3] and head and neck cancers.[4] Currently, in the first-line treatment for P/R/M cervical cancer, pembrolizumab is recommended for programmed death-ligand 1 (PD-L1)-positive patients.[5] However, only a small subset of PD-L1-positive patients benefits from PD-1 inhibitor therapies.[6,7] As such, considerable interest exists in pursuing other novel therapeutic combinations that might have improved clinical benefit through the use of complementary agents with minimal concurrent toxicity profiles, and those mainly include the combination of immune checkpoint blockade with the use of oncolytic viruses.

Oncolytic viruses provide novel and promising therapeutic options for patients with cancers resistant to traditional therapies. They directly lyse tumor cells while keeping normal cells alive, and indirectly potentiate antitumor immunity by releasing antigens and activating inflammatory responses in the tumor microenvironment (TME).[8] Oncolytic virotherapy can improve the efficacy of anti-PD-1 therapy by changing the TME, such as by increasing $CD8^+$ T cells infiltration, elevating PD-L1 expression, and inducing IFN-γ production after T-VEC treatment.[9,10] Research showed that combination therapy can have greater antitumor activity without additional safety concerns.[11] Recombinant human adenovirus type 5 (H101) is a genetically modified oncolytic adenovirus which can selectively replicate in p53-mutant tumors and induce p53 amplification during replication, leading to direct and selective cytotoxicity of tumor cells. Since p53 is the most frequently mutated gene in human cancers, H101 has exhibited anticancer properties in a variety of cancers, such as head and neck carcinoma, gastric cancer, and hepatocellular carcinoma.[12–14] In addition, H101 has been proven to reverse the drug resistance of lung cancer to immune checkpoint inhibitors.[15] In our previous retrospective study, H101 monotherapy or combined with radiotherapy showed promising efficacy in P/R/M gynecologic malignancies without additional adverse events (AEs).[16] However, the specific mechanism for H101 action in cervical cancer is not clearly understood.

Existing data implicated that the pathogenesis of cervical carcinomas is related to somatic mutations in PIK3CA, PTEN, TP53, STK11, and KRAS as well as several copy number alterations.[17] At present, there is a paradigm shift towards developing targeted treatment agents and personalizing cancer treatment. For example, the Molecular Analysis for Therapy Choice (MATCH) study, a tumor-agnostic platform trial that enrolls patients in targeted therapies based on matching genomic alterations, indicated that 28.4% of patients with cervical cancer had an actionable molecular alteration, suggesting a promising future role for treatment stratification directed by genomic testing.[18] However, the mutation profiles associated with H101 therapy have not been fully elucidated. In this study, P/R/M cervical carcinoma patients were recruited and whole exome sequence (WES) was performed for the tumor tissues and paired blood samples. To our knowledge, this is the first study to investigate the predictive value of mutational landscape for cervical cancer patients that received H101 treatment.

Materials and Methods

Study Design and Patients

Patients with histopathologically confirmed P/R/M cervical carcinoma were recruited at the First affiliated hospital of Xi'an Jiaotong University (Xi'an, China). Patients who had received at least one line of systemic therapy or could not tolerate chemotherapy were eligible. Patients should have at least one lesion that allowed for intra-tumoral injections, including direct injection, ultrasound-guided injection, or CT-guided injection, and an Eastern Cooperative Oncology Group performance status score of 0 to 3. Patients meeting any of the following criteria were excluded: 1) Active bacterial, fungal, or viral infections; 2) Active or previously documented autoimmune or inflammatory disorders; 3) Immune-deficiency states; 4) Received of live, attenuated vaccine within 28 days before the first dose of H101; 5) Unresolved toxicity from a previous anticancer therapy, grade 0 or 1.

Paired tumor tissues collected pre- and post-H101 treatment were obtained from patients. Additionally, blood samples for germline analysis from each patient were obtained. This study was approved by the Ethics Committee of Xi'an Jiaotong University (No. XJTU1AF2021LSK-310). All patients signed an informed consent form and approved the sample collection and testing for scientific purposes.

Drug Administration

H101 was injected into target lesions daily for 5 consecutive days per week for 3 weeks as a treatment cycle (1–4 cycles in total). The injection dosage of H101 was determined according to the sum of the diameter (SOD, longest diameters for lesions) of all injected lesions. If the target tumors were stereoscopic, 5.0×10^{11} virus particles (VP) for SOD≤3 cm, 1×10^{12} VP for SOD between 3–5 cm, and 1.5×10^{12} VP for SOD>5 cm. If it was a superficial lesion with a depth of less than 1 cm, 5.0×10^{11} VP for SOD≤5 cm and 1×10^{12} VP for SOD>5cm. Patients received either H101 alone or in combination with radiation and other medications, depending on their specific conditions. H101 treatment was discontinued if one of the following criteria was met: 1) The target lesion increased and progressive disease (PD) was confirmed; 2) Complete disappearance of all clinical and radiographic evidence of disease; 3) Grade 3–5 allergic reaction to the treatment or its excipients, or any treatment-related grade 4 adverse effect; 4) Patient requested to discontinue treatment and retracted the informed consent.

Clinical Assessment

Responses were evaluated by investigators per RECIST v1.1 using CT or magnetic resonance imaging at baseline, every 2 cycles, and every 12 weeks thereafter. Patients with complete response (CR) and partial response (PR) were defined as responders, and patients with stable disease (SD) and PD were defined as non-responders. Objective response rate (ORR) was defined as the percentage of all patients with CR and PR, and disease control rate (DCR) was defined as the percentage of all patients with CR, PR, and SD. Overall survival (OS) was defined as the time from the first use of H101 to death from any cause and progression-free survival (PFS) was defined as the time from the date of the last administration of H101 to disease progression or death from any cause. AEs were recorded during treatment and within 3 months from the end of H101 treatment, and were monitored according to the National Cancer Institute Common Terminology Criteria for Adverse Events (CTCAE, version 5.0).

Whole Exome Sequencing (WES)

Tumor tissue samples and paired peripheral blood samples (considered the normal control) from patients with P/R/M cervical carcinoma were collected for WES. All tumor tissues contained at least 80% malignant cells. The mean sequencing depth of the fresh frozen tissue samples and normal blood were 300 × and 100×. DNA libraries were constructed through the Agilent SureSelect Human All Exon V6 kit (Agilent Technologies, Santa Clara, CA). The samples were sequenced on an Illumina NovaSeq6000 platform (Illumina, Inc.).

Mutation and Copy Number Variations (CNVs) Evaluation

The sequencing data were converted to Fastq file format. Fastq data were evaluated using the FastQC tool. After trimming, the clean data were aligned to the human reference genome hg19 using Burrows-Wheeler Aligner (BWA, version 0.7.12). The comparison result, a binary bam compressed file, was viewed with the Integrative Genomics Viewer (IGV) tool. HaplotypeCaller, an analysis tool of Genome Analysis Toolkit (GATK) (version 3.5), was used to detect variations of the comparison result in the target region, including single nucleotide variant (SNV), insertion/deletion variant (InDel) and copy number variation (CNV). Somatic mutation sites were analyzed using GATK's module MuTect2, annotated using ANNOVAR, counted in Python/Perl, and plotted in R (Version 4.2.0).

Tumor Mutation Burden (TMB) Calculation

TMB was defined as the number of somatic mutations per megabase of the genome region examined. To calculate the TMB, the total number of non-synonymous mutations (including missense, frameshift, nonsense, nonstop, and splice-site) was divided by the length of the total genomic target regions captured with the exome assay.

Microsatellite Instability (MSI) Assessment

MSIsensor and MSIseq were utilized to determine the MSI status of the samples. The MSIsensor software calculated the somatic microsatellite variants by comparing bam files of total WES data from case samples and normal control samples.

The MSIseq software used data on somatic mutations (SNV and InDel) as input files to calculate differences in microsatellite loci from the bam files of normal control and case samples.

Clonal Evolution Analysis

PyClone, based on the Bayesian clustering method, was used to classify somatic mutations with sampling-sequencing depth of one or more sites as putative clone clusters, to estimate the cellular prevalence of these clusters, and to explain the allele imbalance caused by CNV and normal cell contamination. According to the allele frequency and copy number of multiple sample mutations, the cellular prevalence of the mutations among different samples could be inferred. Each cluster included mutations that varied consistently in the proportions of clones across the sample. To investigate the change in mutation frequency in P/R/M cervical carcinoma before and after treatment with H101, PyClone was used to infer the cellular prevalence of mutations. Clonal phylogeny was visualized using Timescape.

Mutational Signature Analysis

To characterize mutational processes operating in P/R/M cervical carcinoma before and after treatment with H101, a mutational signature analysis was performed. A Bayesian variant of the non-negative matrix factorization (NMF) algorithm was applied to analyze mutation counts, which were stratified by 96 tri-nucleotide mutational contexts. The distribution of six types of SNVs (T>A, T>C, C>G, C>A, C>T, and T>G) was analyzed.

Statistical Analysis

Data analyses were performed with SPSS version 22.0 (SPSS Inc. IBM Corp). Categorical data were presented as frequencies and percentages, while continuous data were presented as medians and ranges unless otherwise noted. OS and PFS were estimated using the Kaplan-Meier method and the treatment effects were assessed with the Log rank test. HRs and 95% CIs were estimated using the Cox regression model. Significant high-frequency mutant genes and mutant signatures were determined by performing a univariate Cox analysis. For all analyses, a P value less than 0.05 was considered statistically significant. The results of the annotations were counted in Python/Perl and plotted in R (Version 4.2.0).

Results

Baseline Characteristics and H101 Treatment Efficacy

The study schedule is illustrated in Figure 1A. From July 2021 to February 2022, 17 P/R/M cervical carcinoma patients were enrolled and received at least 1 cycle of H101-based treatment. Patient baseline characteristics are shown in Table 1. The median age was 53 years (range, 43–78 years), and more than half of all patients had an Eastern Cooperative Oncology Group performance status of 1 (70.6%). The histologic breakdown was squamous cell carcinoma (76.5%) and adenocarcinoma (23.5%) (Table 2). The reason for patients to receive H101 intra-tumor injections were persistent lesions after radical concurrent chemoradiotherapy (52.9%), recurrence or metastasis after previous treatment (41.2%), or refractory disease (5.9%). All except one patient had prior radiation exposure, and 8 patients (47.1%) had received bevacizumab as part of a previous therapeutic regime. 8 patients received H101 monotherapy, 6 patients received H101 combined with interstitial brachytherapy, and 3 patients received H101 combined with paclitaxel and platinum-based chemotherapy. There were no new safety signals, and the toxicity profile was aligned with that of previous reports (Table S1). The most common injection site was the cervix, and then the vagina, which can be injected into directly. Only one patient had recurrent lesions in the corpus uteri, so CT simulation was used for the H101 injection.

Most patients showed a decreased tumor load from baseline and the changes in tumor size over time are shown in Figure 1B, whereas the clinical response and duration of response are presented in Figure 1C. At the data cut-off (February 1st, 2023), all patients were evaluated for response with a median follow up of 14 months (range, 5–18 months). 9 patients achieved CR, 3 patients achieved PR, and 2 patients had SD, resulting in an ORR of 70.6% (95% CI: 46.4%-96.7%) and a DCR of 82.4% (62.1%-102.6%) (Table 2). Among all enrolled patients, 2 patients had non-target lesions, and the response for non-injected lesions was SD (Patients 1 and 7). Among all enrolled patients (n=17), 6

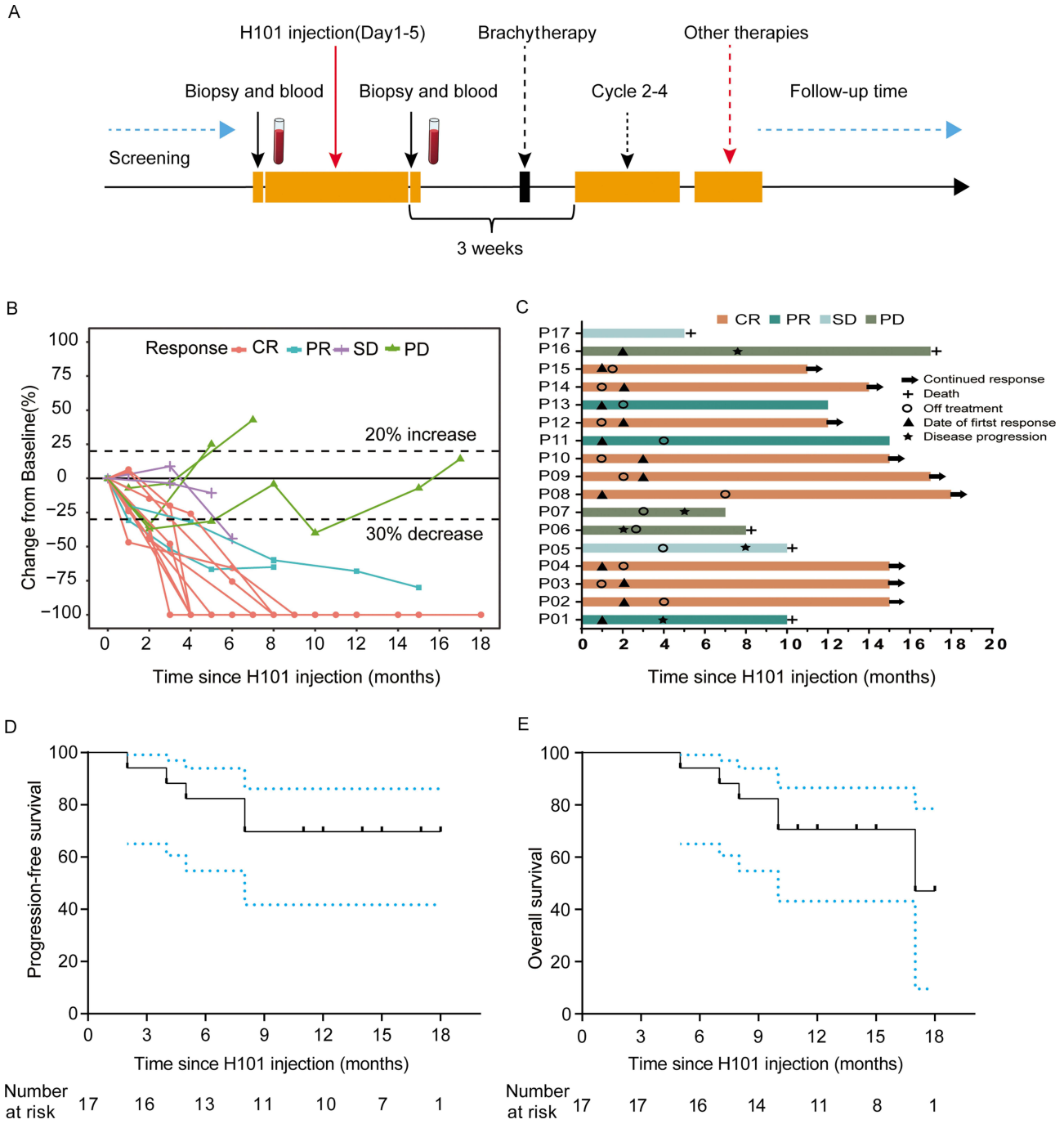

Figure 1 (**A**) Overview of study schedule; (**B**) spider plots to illustrate the tumor burden changes over time; (**C**) swimmer plot showing a clinical response, duration of response, and therapy. (**D**) Kaplan-Meier curve for PFS; (**E**) Kaplan-Meier curve for OS.
Abbreviations: PFS, progression-free survival; OS, overall survival.

patients had died, and 11 patients continued follow up at the data cut-off point. The Kaplan-Meier curve for PFS and OS are shown in Figures 1D and E, and the 1-year PFS and OS rate was 69.7% and 70.6%, respectively.

Correlation Analysis Between the TMB, MSI, and Clinical Efficacy

The analysis of tumor somatic mutations indicated that there were no significant differences in the number of mutations and non-synonymous SNVs between the two groups (*t*-test, $P>0.05$, Figures 2A and B). The mean TMB before and after H101 treatment was 6.1 and 5.4 mutations per megabase, respectively ($P=0.66$) (Figure 2C). The impact of TMB on

Table 1 Baseline Characteristics of Patients

Patient Characteristics, Median (IQR), no. (%)	N=17
Age (years)	53 (43–78)
ECOG performance-status score	
1	12 (70.6)
2	2 (11.8)
3	3 (17.6)
Tumor stage	
I–II	8 (47.1)
III–IV	9 (52.9)
Tumor grade	
1	5 (29.4)
2	7 (41.2)
3	3 (17.6)
Unknown	2 (11.8)
Pathological type	
Squamous cell carcinoma	13 (76.5)
Adenocarcinoma	4 (23.5)
Morbid state at enrollment	
Persistence	9 (52.9)
Recurrence or metastasis	7 (41.2)
Refractory	1 (5.9)
Cycle number of H101	
1	7 (41.2)
≥2	10 (58.8)
Therapy method	
H101 monotherapy	8 (47.1)
Combination therapy	9 (52.9)
Injection site	
Cervix	11 (64.7)
Corpus uteri	1 (5.9)
Vagina	5 (29.4)
Prior radiotherapy	16 (94.1)
Prior systemic chemotherapies (cycles)	
≤4	6 (35.3)
>4	11 (64.7)

outcomes was analyzed. The median value of TMB before H101 treatment was 4 mutations per Mb. According to the median value of TMB, patients were divided into high TMB (TMB-H, TMB>4) and low TMB (TMB-L, TMB≤4) groups. There were 10 (58.8%) patients with TMB-H and 7 (41.2%) patients with TMB-L before treatment. Among the patients with TMB-H, 50% (5/10) patients responded to H101-containing treatment, while all patients in the TMB-L group responded to H101-containing treatment, with a statistically significant difference (P=0.044, Figure 2D), suggesting that patients with TMB-L may benefit more readily from the H101-containing treatment. In addition, survival analysis indicated that TMB-H in patients was associated with lower PFS (HR 1.433, 95% CI: 1.053–1.95, P=0.022) and OS (HR 1.151, 95% CI: 1.033–1.282, P=0.011).

MSI index, caused by defective mismatch repair (MMR) genes, is closely related to the occurrence of tumors. MSI has been clinically used as an important molecular hallmark to determine the prognosis and choose adjuvant therapy in solid tumors. There were 6 patients with high MSI (MSI-H) and 11 patients with non-MSI-H before treatment. Of the patients with MSI-H, 4 patients responded to H101-containing treatment (Responder) and 2 patients did not respond to H101-containing treatment (Non-responder); in patients with non-MSI-H, 8 patients were Responders and 3 patients were Non-responders.

Table 2 MSI Status and H101-Containing Treatment Response

Patient No.	MSI Status	Pathology	Injected Site	Response
1	MSI-H	Adenocarcinoma	Cervix	PR
2	Non-MSI-H	Squamous cell carcinoma	Cervix	CR
3	MSI-H	Squamous cell carcinoma	Cervix	CR
4	Non-MSI-H	Squamous cell carcinoma	Vaginal	CR
5	Non-MSI-H	Squamous cell carcinoma	Vaginal	SD
6	MSI-H	Squamous cell carcinoma	Cervix	PD
7	Non-MSI-H	Squamous cell carcinoma	Cervix	PD
8	Non-MSI-H	Squamous cell carcinoma	Cervix	CR
9	Non-MSI-H	Squamous cell carcinoma	Vaginal	CR
10	Non-MSI-H	Adenocarcinoma	Cervix	CR
11	Non-MSI-H	Adenocarcinoma	Vaginal	PR
12	MSI-H	Adenocarcinoma	Cervix	CR
13	Non-MSI-H	Squamous cell carcinoma	Vaginal	PR
14	Non-MSI-H	Squamous cell carcinoma	Cervix	CR
15	MSI-H	Squamous cell carcinoma	Cervix	CR
16	Non-MSI-H	Squamous cell carcinoma	Cervix	PD
17	MSI-H	Squamous cell carcinoma	Corpus uteri	SD

Abbreviations: MSI, microsatellite instability; MSI-H, high microsatellite instability; CR, complete response; PR, partial response; PD, progressive disease; SD, stable disease.

Herein, the association between MSI and the efficacy of H101-containing treatment was investigated (P=0.528, Figure 2E), suggesting that there is no significant relationship between the efficacy response of H101-containing treatment for P/R/M cervical carcinoma and MSI status.

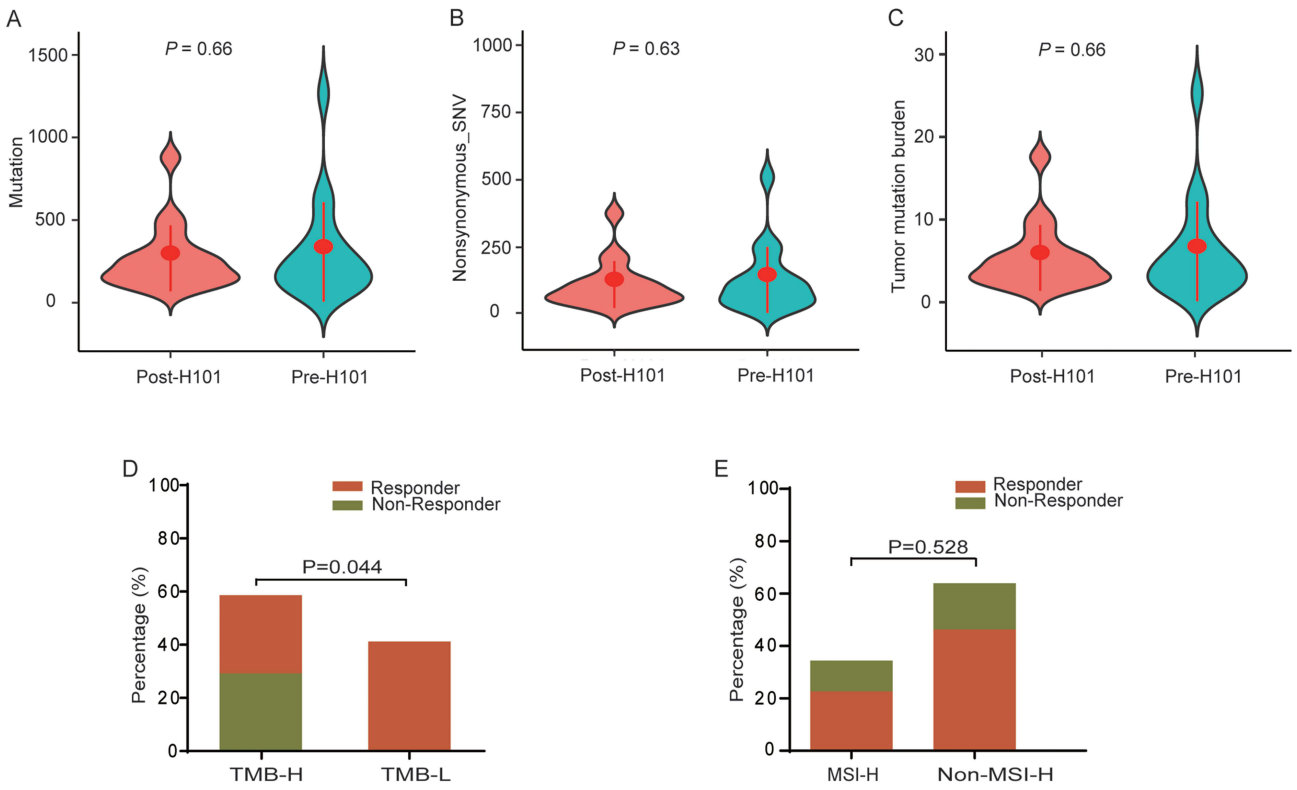

Figure 2 Genomic architecture in the tumor samples before and after H101-containing treatment. (**A**) Mutations; (**B**) non-synonymous-SNVs; (**C**) total TMBs. (**D**) The association between TMB and the response rate of H101-containing treatment. (**E**) The association between MSI and the response rate of H101-containing treatment.
Abbreviations: TMB, tumor mutation burden; MSI, microsatellite instability.

https://doi.org/10.2147/DDDT.S429180

Analysis of High-Frequency Mutation Genes and Response to Treatment

The general mutational landscape of the tumor tissue samples from 17 P/R/M cervical carcinoma patients before and after H101-containing treatment is displayed in Figure 3. The missense mutation was the most common variant classification (Figure 3A). Single nucleotide polymorphisms (SNPs) were the dominant mutation type (Figure 3B). C>T transition was the highest mutation type (Figure 3C). The median of variant counts was 95.5 (Figure 3D). Figure 3E uses a boxplot to display the mutation number in different mutation classification, the number of missense mutations was the highest compared with other mutations (Figure 3E). Top 10 mutated genes were identified (Figure 3F), including DDX5, TTN, MPO, THEMIS2, ACTB, KMT2D, RPS6, ALDOA, PTPN23, and DGKZ. Among the top 10 mutated genes, the mutation classification of TTN, THEMIS2, KMT2D, and PTPN23 were missense mutations, and DDX5, MPO, ACTB, RPS6, ALDOA, and DGKZ were splice-site mutations.

Identification of High-Frequency Mutation Genes with Function Change in Response to Treatment

The oncoprint map of the top 30 mutated genes with function change is shown in Figures 4A and B. Nonsense mutations and frameshift mutations are pathogenic somatic mutations, and loss of function is the most common pathogenic mechanism. Non-synonymous in TTN, KMT2D, DNAH7, ADAP1, ACTB, PTPN23 and THEMIS2, non-frameshift

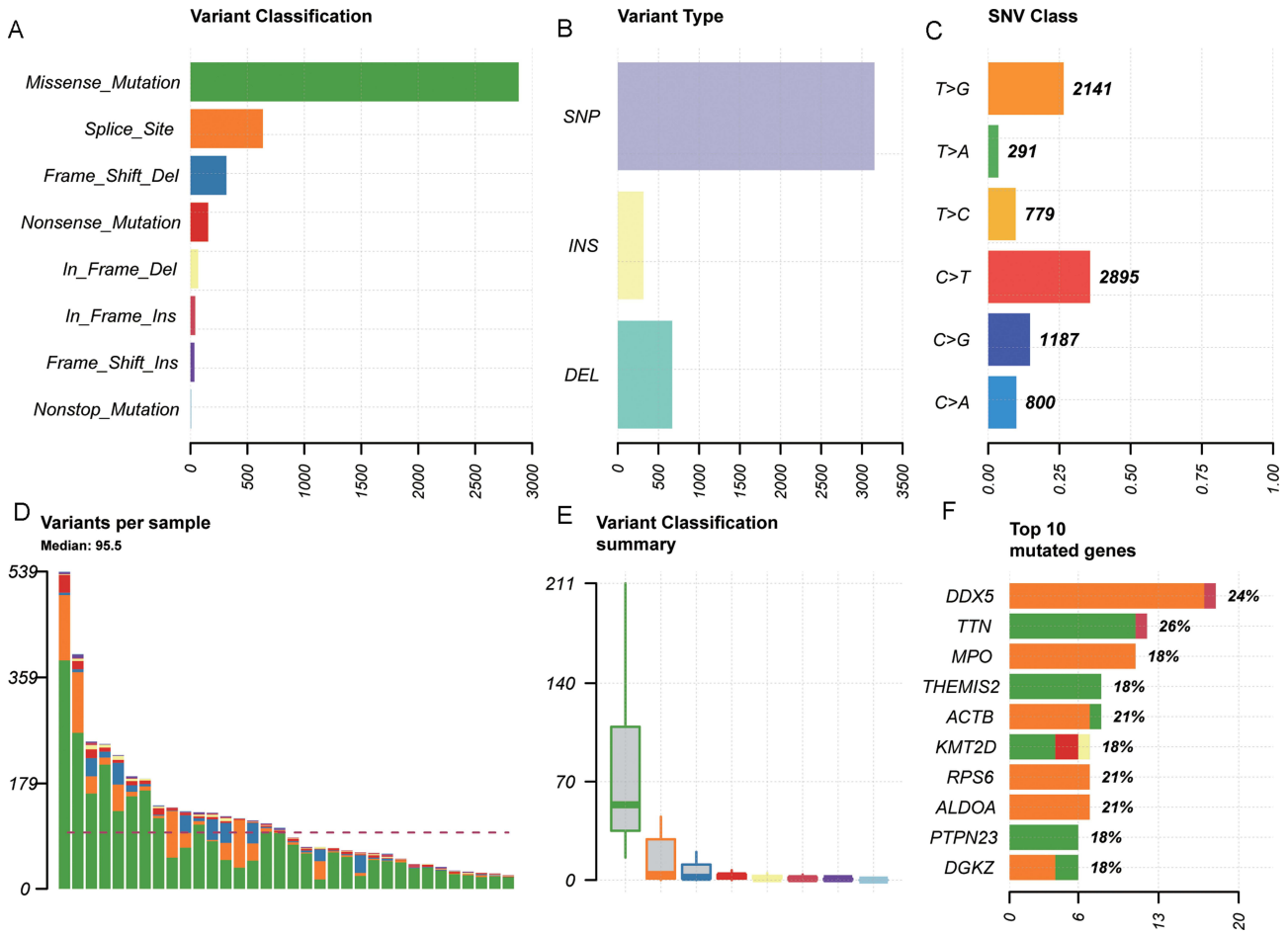

Figure 3 The general mutational landscape of tumor tissue samples from 17 cervical carcinoma patients before and after H101-containing treatment. (**A**) Variant classification. X-axis and Y-axis respectively represent the number of variants and variant classification. (**B**) Variant type. X-axis and Y-axis respectively represent the number of variants and variant types. (**C**) SNV class. X-axis and Y-axis respectively represent the ratio and SNV class. The number on the right represents the number of SNV classes. (**D**) Variants per sample. The X-axis and Y-axis respectively represent the sample and number of variants. (**E**) Boxplots for variant classification summary. X-axis and Y-axis respectively represent variant classification and the number of variant classifications. (**F**) Top 10 mutated genes. X-axis and Y-axis respectively represent the number of variants and mutated genes. The number on the right represents the percentage of mutated genes.

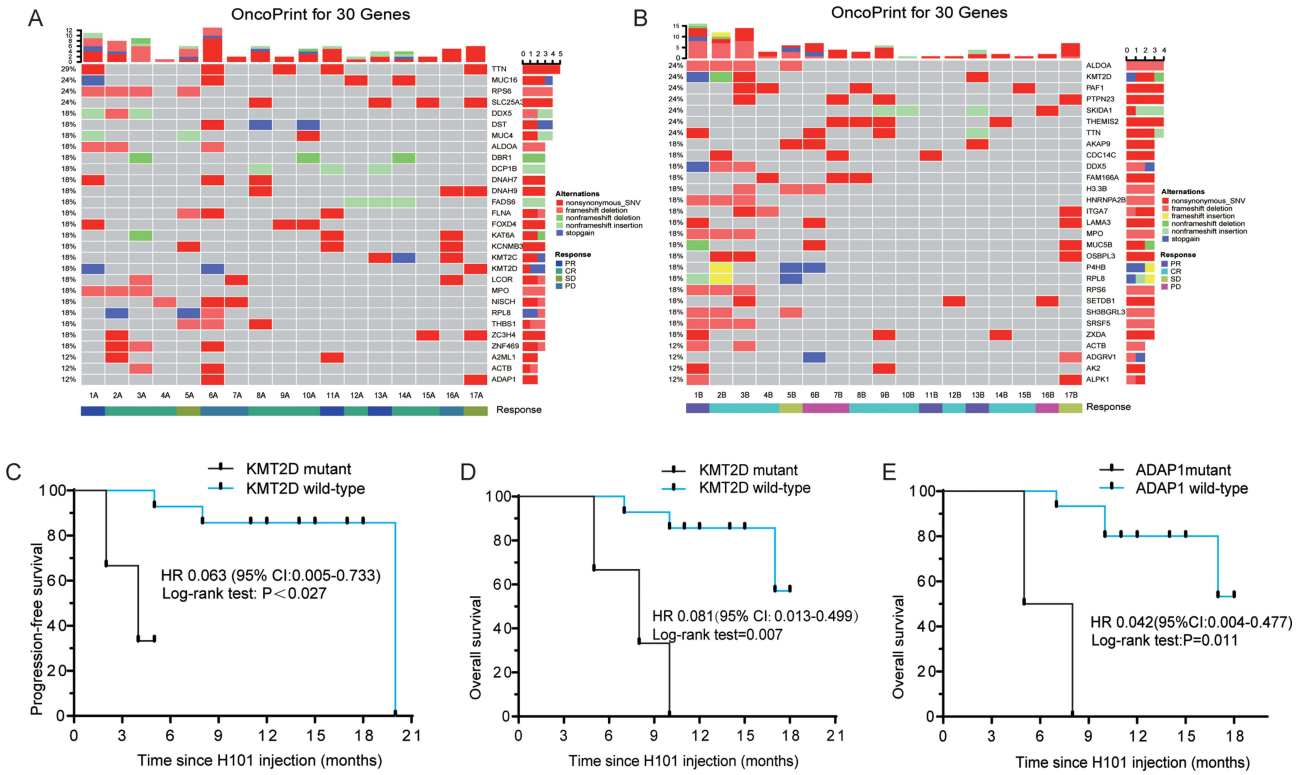

Figure 4 Genomic landscape of P/R/M cervical cancer patients treated with H101. (**A**) Oncoprint of mutations in the top 30 mutated genes in tumor tissue samples from 17 cervical carcinoma patients before H101-containing treatment. (**B**) Oncoprint of mutations in the top 30 mutated genes in tumor tissue samples from 17 cervical carcinoma patients after H101-containing treatment. The row and column respectively represent mutated genes and samples. Different colors represent different mutation types, and gray represents no mutation. The panels on the right side represent the number of samples with mutations in the corresponding gene. (**C**) Kaplan-Meier curve of KMT2D mutant for PFS. (**D**) Kaplan-Meier curve of KMT2D mutant for OS. (**E**) Kaplan-Meier curve of ADAP1 mutant for OS.
Abbreviations: PFS, progression-free survival; OS, overall survival.

insertion mutation in TTN, frameshift deletion mutation in ALDOA and ACTB, stop-gain mutation in KMT2D, frameshift deletion mutation in ALDOA, and non-synonymous mutation in DNAH7, ADAP1, PTPN23, and THEMIS2 were observed in patients. A non-synonymous mutation in DNAH7 was found in 3 patients (Patients 1/6/8) before treatment, and a non-synonymous mutation in ADAP1 was found in 2 patients (Patients 6/17) before treatment, which all disappeared after treatment, suggesting that DNAH7 and ADAP1 maybe pre-treatment-specific genes. In addition, the presence of ADAP1 mutation in patients before treatment with poor response suggests that ADAP1 may be associated with resistance to H101 treatment. Among the genes mentioned above, a mutation in four genes (TTN, ALDOA, KMT2D, and ADAP1) was present in Patients 6 and 17 before treatment, corresponding to non-responsive treatment. KMT2D mutation was associated with shorter PFS (HR 0.063, 95% CI: 0.005–0.733, P=0.027) and shorter OS (HR 0.081, 95% CI: 0.013–0.499, P=0.007) after H101-containing treatment (Figures 4C and D). ADAP1 mutation was associated with shorter OS (HR 0.042, 95% CI: 0.004–0.477, P=0.011), but had no obvious correlation with PFS (P=0.159) (Figure 4E).

Analysis of Clonal Evolution and Response to Treatment

Phylogenetic trees were constructed with the method of maximum likelihood (Figure S1). The cellular prevalence plots provided a profile of all sub-clones and indicated the changing sub-clonal compositions among samples from each patient's tumor (Figure 5). The results indicated that H101 treatment often resulted in substantial changes in the relative proportions of individual sub-clones or clusters within the primary tumor. A total of 40 clusters in Patient 1, 12 clusters in Patient 14, 11 clusters in Patient 17, and 10 clusters in Patient 6 were detected, indicating evident tumor heterogeneity in the above 4 patients (Figures 5A-D). In Patient 12, with 6 clusters, the cellular prevalence of Cluster 1 went from near zero to near 0.2, and the cellular prevalence of Cluster 4 went from near 0.25 to near zero (Figure 5E). A mutation in PTPN23 was present in Patients

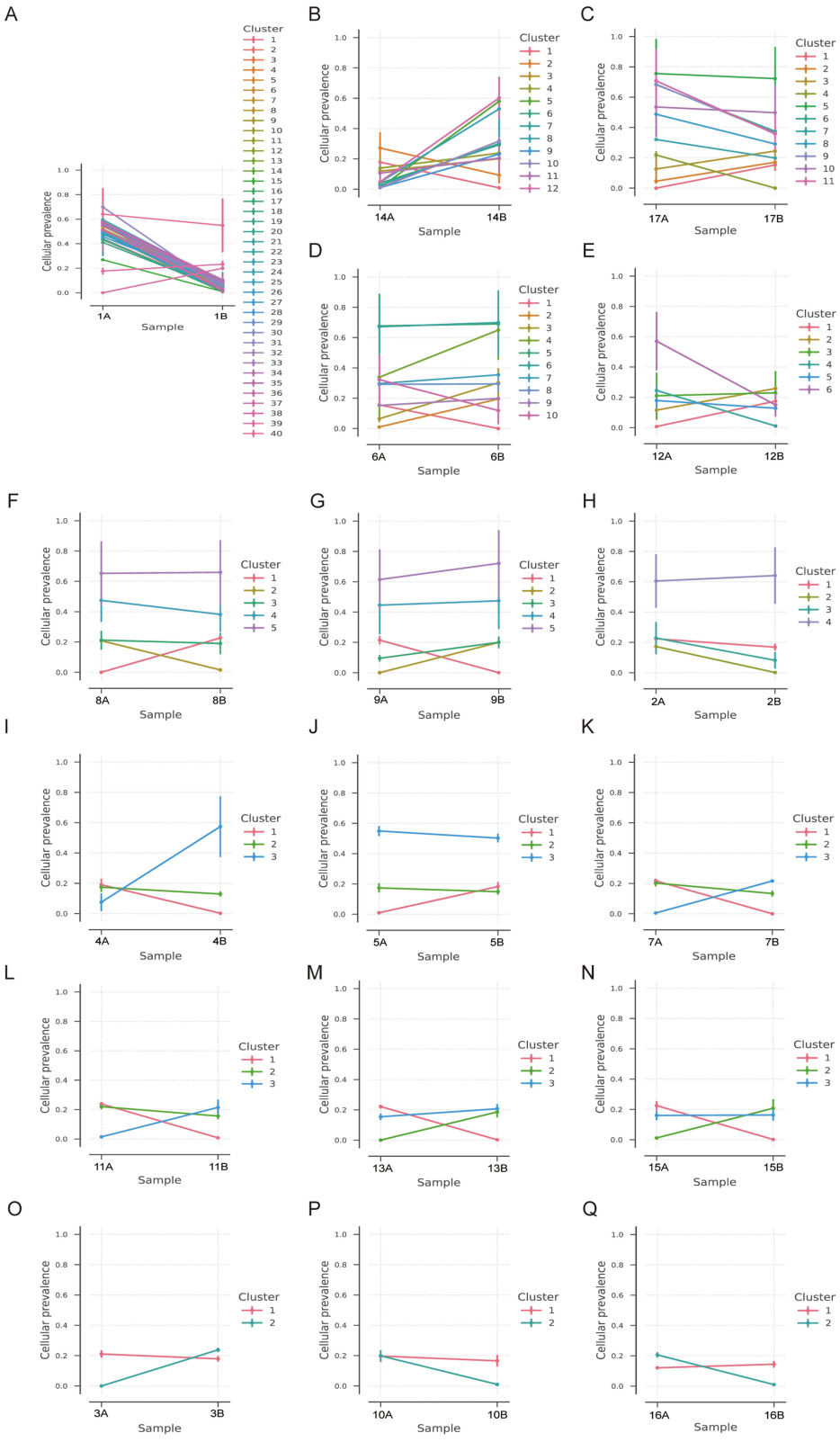

Figure 5 Clonal evolution analysis in patients before and after H101-containing treatment, showing the cellular prevalence of mutations after clustering. (**A**) Patient 1. (**B**) Patient 14. (**C**) Patient 17. (**D**) Patient 6. (**E**) Patient 12. (**F**) Patient 8. (**G**) Patient 9. (**H**) Patient 2. (**I**) Patient 4. (**J**) Patient 5. (**K**) Patient 7. (**L**) Patient 11. (**M**) Patient 13. (**N**) Patient 15. (**O**) Patient 3. (**P**) Patient 10. (**Q**) Patient 16.

12/9/7, gained in Cluster 2 of Patient 9 and Cluster 3 of Patient 7 after treatment. A mutation in PTPN23 appeared in Cluster 5 of Patient 12, and the cloning pattern of Cluster 5 did not change before and after treatment. These findings may indicate that H101-containing treatment can affect mutations in PTPN23. Patients 8 and 9 had 5 clusters. Cluster 1 in Patient 8 was acquired after treatment, Cluster 2 disappeared after treatment, and the opposite was true in Patient 9 (Figures 5F and G). A mutation in NCOR2 was present in Cluster 1 of Patient 8 and Cluster 2 of Patient 9, suggesting that NCOR2 mutations may be a molecular indicator of the efficacy of H101 treatment. Patient 2 had 4 clusters, of which Cluster 2 disappeared after treatment (Figure 5H). A mutation in TUT1 was present in Patients 2/9, and mutations in LINC00564, DTWD2, and CHCHD3 were present in Patients 1/2/3. Mutations in TUT1, LINC00564, and CHCHD3 were present in Cluster 1 of Patient 2, a mutation in TUT1 was present in Cluster 1 of Patient 9, and mutations in LINC00564 and CHCHD3 were present in Cluster 1 of Patient 3. A mutation in DTWD2 was found in Cluster 2 of Patient 2 before treatment, Cluster 2 of Patient 3 after treatment, and Cluster 38 of Patient 1. These findings suggest that mutations in LINC00564 and CHCHD3 may not be related to H101-containing treatment, while TUT1 and DTWD2 may be sensitive genes to H101-containing treatment. Three clusters were present in Patients 4/5/7/11/13/15, suggesting that this clonal composition may be the main pattern of P/R/M cervical cancer patients (Figures 5I–N). A mutation in TRPC4AP was present in Patients 4/13, and mutations in CACNA2D4 and MFSD2A were found in Patients 11/13. Mutations in TRPC4AP, CACNA2D4, and MFSD2A were present in Cluster 1 of Patient 13, which disappeared after treatment. A mutation in CACNA2D4 was detected in Cluster 3 of Patient 11 before treatment, a mutation in MFSD2A was detected in Cluster 2 of Patient 11 before treatment, and a mutation in TRPC4AP was detected in Cluster 2 of Patient 4 before treatment. A mutation in CACNA2D4 may be affected by H101-containing treatment. Two clusters were present in Patients 3/10/16, in which Cluster 2 disappeared in Patient 10/16 after treatment, and acquired in Patient 3 after treatment (Figures 5O–Q). A mutation in PKHD1L1 was present in Patients 1/9/14/17. A PKHD1L1 mutation existed in Cluster 31 of Patient 1 before treatment, and Cluster 31 was significantly reduced after treatment. A PKHD1L1 mutation was detected in Cluster 5 of Patient 9 after treatment, and there was no significant change in Cluster 5 before and after treatment. PKHD1L1 mutation was present in Cluster 9 of Patient 14, and Cluster 9 was obtained after treatment. In Patient 17, a PKHD1L1 mutation was found in two different clusters (8 and 9), and no significant changes were observed in these clusters before and after treatment. A TTN mutation was detected in Patients 1/9/6/7/17, among which a TTN mutation was in Cluster 38 with increased cell prevalence after treatment and Cluster 18 with reduced cell prevalence after treatment of Patient 1. A TTN mutation was present in Cluster 18 of Patient 9 with increased cell prevalence after treatment, Cluster 1 with increased cell prevalence, and Cluster 9 with reduced cell prevalence after treatment of Patient 6. In addition, a TTN mutation was present in Cluster 3 of Patient 7 with increased cell prevalence after treatment, and Cluster 7 and 8 in Patient 17 with increased cell prevalence after treatment. These results indicated that the change in tumor heterogeneity caused by a TTN mutation may be related to resistance to H101-containing treatment.

In summary, 15 patients were with clusters that were acquired after treatment. These results suggested that sub-clonal populations may be selectively altered following H101-containing treatment, which can change tumor heterogeneity in patients with P/R/M cervical cancer.

Analysis of Mutational Signature and Response to Treatment

The distribution of six subtypes of base substitutions (C>A, C>G, C>T, T>A, T>C, and T>G) in the SNVs were analyzed to elucidate how mutational signatures evolve in H101-containing treatment for P/R/M cervical carcinoma. 4 mutational signatures were identified in the tumors of patients before treatment using the TCGA database (Signatures 1A, 2, 17, and U1) and 3 in tumors of patients after treatment (Signatures 1A, 13, and U1) (Figures 6A and B). In tumor samples with good treatment effect (CR and PR) and TCGA database, 4 mutational signatures were identified (Signatures 1A, 2, 17, and U1) and 3 in samples with poor effect (PD and SD) and TCGA database (Signatures 1A, 2, and U1) (Figures 6C and D). Signature 1A, characterized by the prominence of C>T substitutions at NpCpG trinucleotides, was observed in 13 patients, except Patients 2/4/8/15 (Figure 6E). Signature 2, characterized by C>T and C>G mutations at TpCpN trinucleotides, was observed in Patients 1/6/14/17 (Figure 6E). Signature 17, characterized by T>C and T>G substitutions at NTT trinucleotides, was present in 11 patients (1/3/7/9/10/11/12/13/14/15/16) but not in Patients 5/6/17 with PD/SD (Figure 6E). Signature U1 was detected in 14 patients, except Patients 1/6/17 (Figure 6E). Univariate Cox regression analysis showed that Signature 2 was a negative prognostic factor for PFS after H101-containing treatment (P=0.044). Patients were divided

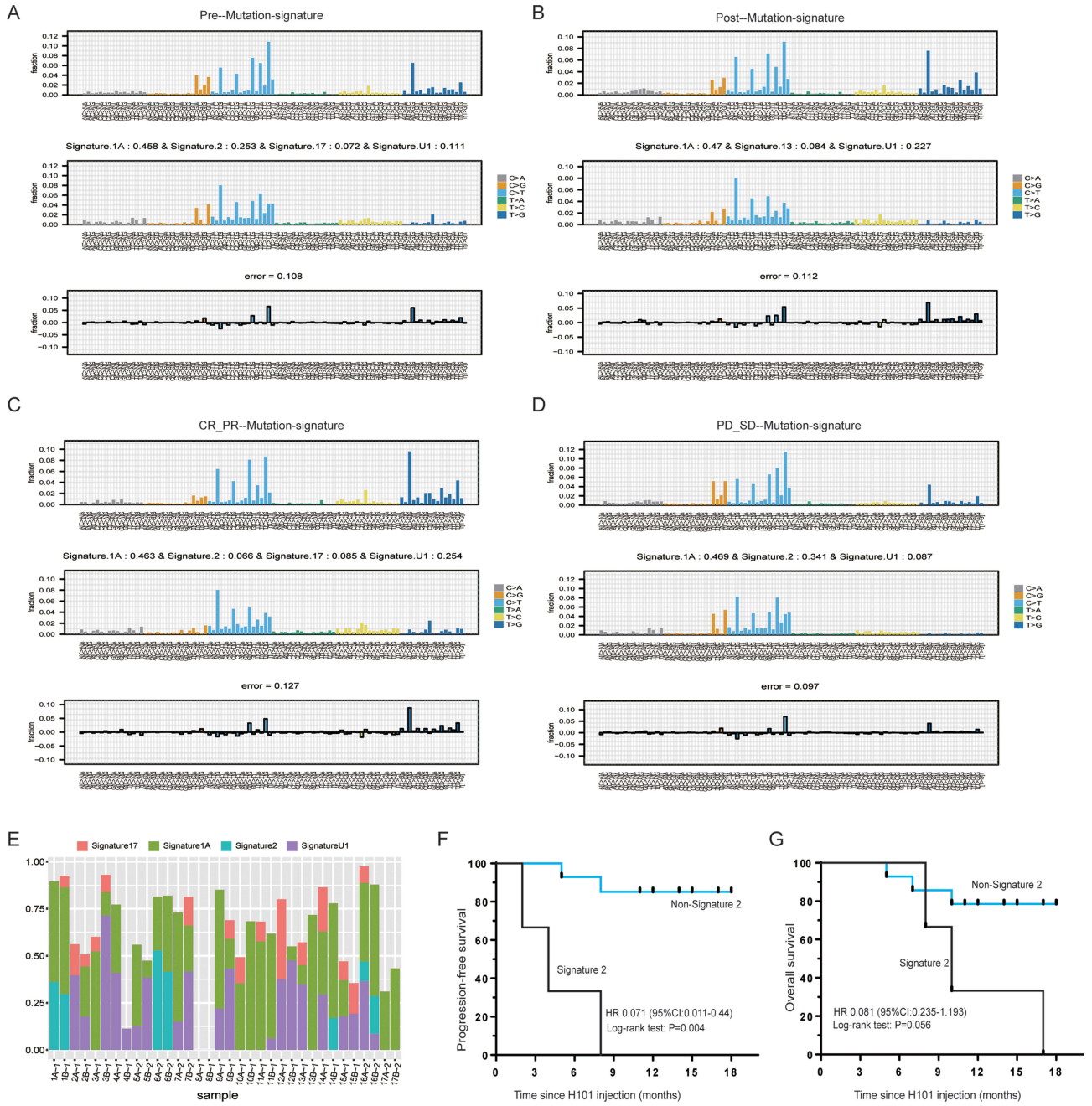

Figure 6 Mutational signature analysis in the tumor samples before and after H101-containing treatment. (**A**) Mutational signature analysis in tumors of patients before treatment and TCGA database. (**B**) Mutational signature analysis in tumors of patients after treatment and TCGA database. (**C**) Mutational signature analysis in tumors of patients with CR and PR, and TCGA database. (**D**) Mutational signature analysis in tumors of patients with PD and SD, and TCGA database. (**E**) Distribution of Signatures 1A, 2, 17, and U1 in patients (Capital A means pre-H101 treatment and capital B means post-H101 treatment; number 1 represents patients with CR and PR, and number 2 represents patients with SD and PR). (**F**) Kaplan-Meier curve for PFS in patients with Signature 2 mutation and Non-signature 2 mutations. (**G**) Kaplan-Meier curve for OS in patients with Signature 2 mutation and Non-signature 2 mutations.

Abbreviations: CR, complete response; PR, partial response; PD, progressive disease; SD, stable disease; OS, overall survival.

into the Signature 2 group and Non-Signature 2 group according to patients with or without Signature 2 mutation. Survival analysis indicated that Signature 2 was associated with shorter PFS (HR 0.071, 95% CI: 0.011–0.44, Log rank test: P=0.004), while the presence of Signature 2 mutation had no significant effect on OS (HR 0.081, 95% CI: 0.235–1.193, Log rank test: P=0.056) (Figures 6F and G).

Discussion

In this study, WES was conducted to prospectively examine genomic profiling of the clinical response to H101 in patients with P/R/M cervical carcinoma. The clinical activity (ORR of 70.6% and DCR of 82.4%) in our 17-patient cohort was well aligned with previously published data (ORR of 72.4%).[16] Further, the correlations between the efficacy of H101 and MSI, TMB, and high-frequency mutated genes, as well as the clonal evolution and mutation signature, were further analyzed to elucidate the alteration caused by H101. To the best of our knowledge, this is the first study on genomic profiling of cervical cancer to identify potential predictors of response to H101 intra-tumor therapy.

The prognosis of cervical cancer patients with P/R/M disease remains very poor, with an estimated OS around 13–17 months.[19] H101 is regarded as a new type of immunotherapy, and there are no clinical studies reported on H101 in the treatment of P/R/M cervical cancer, except for our previous retrospective study.[16] There have been several studies on monotherapy or combination therapy with immune checkpoint inhibitors for P/R/M cervical cancer. In the Phase III EMPOWER trial involving patients with recurrence/metastatic cervical cancer that progressed after platinum-based chemotherapy, cemiplimab monotherapy demonstrated an increased ORR (16.4% vs 6.3%) and prolonged OS (12.0 vs 8.5 months) as compared with chemotherapy.[20] In addition, sintilimab plus anlotinib yielded an ORR of 54.8% with a DCR of 88.1%.[21] Our results (ORR, DCR) are comparable with those of sintilimab, a monoclonal antibody against PD-1, plus anlotinib, a multi-kinase inhibitor,[21] and aligned with our previous retrospective study.[16] Although the median follow-up time of 14 months is insufficient for survival analysis, it is appropriate to evaluate gene mutations and responses before and after H101 treatment.

Previous data have shown that virotherapy can promote intra-tumoral T-cell infiltration, and turn cold tumors warm by changing the TME, thus potentiating antitumor immunity.[9,22] Moreover, compelling evidence has been added by a recently published work, in which Prof. Chen et al proposed that it is an attractive strategy to use these agents to convert "missing-target" TME types (I, III, and IV) into type II, making them susceptible to anti-PD therapy.[23] Therefore, oncolytic virus therapy is considered a new type of immunotherapy. TMB and MSI have been identified as predictive biomarkers for immunotherapy.[24,25] However, whether these biomarkers can predict the efficacy of the oncolytic virus has not been reported. In this study, we found that TMB-L patients were more likely to respond to H101 and had better survival (P=0.044), while the H101 response rate between MSI-H patients and non-MSI-H patients was not significantly different (P=0.528). The finding is exactly the opposite of what is seen with immune checkpoint inhibitor (ICI) treatment of cervical cancer (ie, the median PFS and OS were longer in patients with TMB-H than in those with TMB-L).[24] TMB and MSI are potential biomarkers for predicting response to ICIs because they are closely related to tumor-specific antigens,[26,27] which is important for ICI therapy. Since the mechanisms of the oncolytic virus are by large both to stimulate antigenic response and to directly lyse tumor cells, its tumorigenic and/or immunogenic response may not be as sensitive as ICIs in association with TMB and MSI.

In addition, we found that some high-frequency mutation genes with functional alterations are associated with the clinical efficacy of H101-containing treatment. These genes include those such as TTN, KMT2D, ALDOA, DNAH7, ADAP1, PTPN23, and THEMIS2. With next-generation sequencing-based genomic profiling analysis, the mutation in TTN was detected in Chinese patients with primary epithelial ovarian cancer.[28] TTN mutations are associated with UBE2T expression, and increased UBE2T expression predicts poor survival in epithelial ovarian cancer.[29] TTN is a highly mutated driver gene in endometrial cancer.[30] Mutated KMT2D was found in gastric-type mucinous carcinoma of the uterine cervix.[31] Low-frequency mutation in KMT2D was observed in vulvar squamous cell carcinoma.[32] A mutation in KMT2D with high mutation frequency was related to higher TMB in cervical cancer.[33] ALDOA promotes the malignant transformation of cervical adenocarcinoma through the modulation of HIF-1α signaling.[34] High expression of ALDOA was related to poor prognosis in breast cancer.[35] A mutation in DNAH7 was reported in male infertility with severe asthenozoospermia.[36,37] ADAP1 was associated with the progression and prognosis of squamous cell carcinoma and lung adenocarcinoma.[38,39] PTPN23 acts as a tumor suppressor gene in intestinal cancer and hepatocellular carcinoma.[40,41] However, there is no report of DNAH7, ADAP1, and PTPN23 in gynecological carcinoma. THEMIS2, also known as C1ORF38/ICB1, was highly expressed in clear cell carcinoma of the ovary and endometrial adenocarcinoma.[42,43]

Herein, non-synonymous and non-frameshift insertion mutation in TTN, stop-gain non-synonymous and non-frameshift insertion in KMT2D, frameshift deletion mutation in ALDOA, and non-synonymous mutation in DNAH7, ADAP1, PTPN23, and THEMIS2 were observed in patients. In addition, our results indicated that the presence of TTN,

ALDOA, KMT2D, and ADAP1 mutation before treatment was associated with poor efficacy of H101-containing treatment. KMT2D and ADAP1 mutations were associated with poor prognosis in P/R/M cervical carcinoma. Clonal evolution analysis indicated that the change in tumor heterogeneity caused by TTN mutation may be related to resistance to H101-containing treatment. Hence, we speculate that TTN, KMT2D, ALDOA, DNAH7, ADAP1, PTPN23, and THEMIS2 may be considered potential therapeutic targets of H101-containing treatment for P/R/M cervical carcinoma.

It has been reported that drug resistance-related mutations may exist in tumors before treatment or occur and accumulate during treatment.[44–47] Different mutation characteristics may be related to the special tumorigenesis and development process. Thus, profiling clonal evolution and mutational signature between tumors before and after H101-containing treatment could reveal putative drivers of resistance to drug treatment. In this study, 4 mutational signatures were identified in tumors of patients before treatment (Signatures 1A, 2, 17, and U1) and 3 in tumors of patients after treatment (Signatures 1A, 13, and U1). In tumor samples with good treatment effect, 4 mutational signatures were identified (Signature 1A, 2, 17, and U1) and 3 in samples with poor effect (Signature 1A, 2, and U1). Signature 1A is likely related to the relatively elevated rate of spontaneous deamination of 5-methyl-cytosine which results in C>T transitions and predominantly occurs at NpCpG trinucleotides.[48] Signature 2, attributed to the over-activity of the APOBEC family of cytidine deaminases, which converts cytidine to uracil and is coupled with the activity of the base excision repair and DNA replication machinery, is enriched in cervical cancer.[17,49,50] Signature 2 disappeared after treatment, suggesting that H101-containing treatment may be related to the activity of APOBEC family members, base excision repair, and DNA replication machinery. In addition, we found that Signature 2 was associated with shorter PFS. 5-fluorouracil treatment induces mutations similar to Signature 17 in human cancer.[51] These findings may provide additional information for prognostic prediction of tolerance to H101-containing treatment.

There are some limitations in this study. Firstly, the small sample size may affect the reliability of our results, and it's difficult for us to do subgroup analysis. A clinical trial with a large sample size has already been registered (ClinicalTrials.gov identifier: NCT05051696), expecting to obtain more convincing evidence. Secondly, though WES may discover more genomic variants relevant to H101-containing treatment resistance, more technologies are needed to uncover the bona fide mechanisms and thus actionable biomarkers in cervical cancer patients appropriate for H101-mediated treatment. The ongoing research using single-cell RNA sequencing and spatial transcriptomics (ST) can provide additional insights to untangle the intricate molecular mechanisms underlying the complex TME.

Conclusion

Our study established, for the first time, a genomic landscape and tumor evolution before and after treatment with H101 for cervical cancer. We explored the potential application of H101 in the treatment of cervical cancer and provided novel insights for individualized and precision medicine. We have probed numerous newly detected somatic mutations, which strengthens our understanding of the somatic mutation patterns upon H101 treatment. In addition, certain mutated genes, including TTN, KMT2D, ALDOA, DNAH7, ADAP1, PTPN23, and THEMIS2, could be considered for future validation as potential therapeutic targets of H101-containing treatment in cervical carcinoma. The genomic characteristics associated with this therapy, such as clonal evolution and mutational signature, are valuable for further investigations.

Data Sharing Statement

The datasets generated and/or analysed during the current study are available in Jianguoyun [https://www.jianguoyun.com/c/sd/176f98a/16c6294baa56a261].

Ethical Approval

This study was approved by the Ethics Committee of Xi'an Jiaotong University (No. XJTU1AF2021LSK-310). All patients signed an informed consent form and approved the sample collection and testing for scientific purposes.

Author Contributions

All authors made a significant contribution to the work reported, whether that is in the conception, study design, execution, acquisition of data, analysis and interpretation, or in all these areas; took part in drafting, revising or critically

reviewing the article; gave final approval of the version to be published; have agreed on the journal to which the article has been submitted; and agree to be accountable for all aspects of the work.

Funding

There is no funding to report.

Disclosure

The authors declare that they have no conflicts of interest in this work.

References

1. Marret G, Borcoman E, Le Tourneau C. Pembrolizumab for the treatment of cervical cancer. *Expert Opin Biol Ther*. 2019;19(9):871–877.
2. Stevanovic S, Draper LM, Langhan MM, et al. Complete regression of metastatic cervical cancer after treatment with human papillomavirus-targeted tumor-infiltrating T cells. *J Clin Oncol*. 2015;33(14):1543–1550.
3. Stevanovic S, Pasetto A, Helman SR, et al. Landscape of immunogenic tumor antigens in successful immunotherapy of virally induced epithelial cancer. *Science*. 2017;356(6334):200–205.
4. Seiwert TY, Burtness B, Mehra R, et al. Safety and clinical activity of pembrolizumab for treatment of recurrent or metastatic squamous cell carcinoma of the head and neck (KEYNOTE-012): an open-label, multicentre, phase 1b trial. *Lancet Oncol*. 2016;17(7):956–965.
5. Gong MN, Bajwa EK, Thompson BT, Christiani DC. Body mass index is associated with the development of acute respiratory distress syndrome. *Thorax*. 2010;65(1):44–50.
6. Chung HC, Ros W, Delord JP, et al. Efficacy and Safety of Pembrolizumab in Previously Treated Advanced Cervical Cancer: results From the Phase II KEYNOTE-158 Study. *J Clin Oncol*. 2019;37(17):1470–1478.
7. Colombo N, Dubot C, Lorusso D, et al. Pembrolizumab for Persistent, Recurrent, or Metastatic Cervical Cancer. *N Engl J Med*. 2021;385 (20):1856–1867.
8. Ma R, Li Z, Chiocca EA, Caligiuri MA, Yu J. The emerging field of oncolytic virus-based cancer immunotherapy. *Trends Cancer*. 2023;9(2):122–139.
9. Ribas A, Dummer R, Puzanov I, et al. Oncolytic Virotherapy Promotes Intratumoral T Cell Infiltration and Improves Anti-PD-1 Immunotherapy. *Cell*. 2017;170(6):1109–1119.e1110.
10. Zhang Y, Qian L, Chen K, et al. Intraperitoneal oncolytic virotherapy for patients with malignant ascites: characterization of clinical efficacy and antitumor immune response. *Mol Ther Oncolytics*. 2022;25:31–42.
11. Chesney J, Puzanov I, Collichio F, et al. Randomized, Open-Label Phase II Study Evaluating the Efficacy and Safety of Talimogene Laherparepvec in Combination With Ipilimumab Versus Ipilimumab Alone in Patients With Advanced, Unresectable Melanoma. *J Clin Oncol*. 2018;36 (17):1658–1667.
12. Mell LK, Brumund KT, Daniels GA, et al. Phase I Trial of Intravenous Oncolytic Vaccinia Virus (GL-ONC1) with Cisplatin and Radiotherapy in Patients with Locoregionally Advanced Head and Neck Carcinoma. *Clin Cancer Res*. 2017;23(19):5696–5702.
13. Zhang R, Cui Y, Guan X, Jiang X. A Recombinant Human Adenovirus Type 5 (H101) Combined With Chemotherapy for Advanced Gastric Carcinoma: a Retrospective Cohort Study. *Front Oncol*. 2021;11:752504.
14. Lin XJ, Li QJ, Lao XM, Yang H, Li SP. Transarterial injection of recombinant human type-5 adenovirus H101 in combination with transarterial chemoembolization (TACE) improves overall and progressive-free survival in unresectable hepatocellular carcinoma (HCC). *BMC Cancer*. 2015;15:707.
15. Zhang QN, Li Y, Zhao Q, et al. Recombinant human adenovirus type 5 (Oncorine) reverses resistance to immune checkpoint inhibitor in a patient with recurrent non-small cell lung cancer: a case report. *Thorac Cancer*. 2021;12(10):1617–1619.
16. Zhang J, Zhang Q, Liu Z, et al. Efficacy and Safety of Recombinant Human Adenovirus Type 5 (H101) in Persistent, Recurrent, or Metastatic Gynecologic Malignancies: a Retrospective Study. *Front Oncol*. 2022;12:877155.
17. Ojesina AI, Lichtenstein L, Freeman SS, et al. Landscape of genomic alterations in cervical carcinomas. *Nature*. 2014;506(7488):371–375.
18. Flaherty KT, Gray RJ, Chen AP, et al. Molecular Landscape and Actionable Alterations in a Genomically Guided Cancer Clinical Trial: national Cancer Institute Molecular Analysis for Therapy Choice (NCI-MATCH). *J Clin Oncol*. 2020;38(33):3883–3894.
19. Cibula D, Pötter R, Planchamp F, et al. The European Society of Gynaecological Oncology/European Society for Radiotherapy and Oncology/ European Society of Pathology Guidelines for the Management of Patients With Cervical Cancer. *Int J Gynecol Cancer*. 2018;28(4):641–655.
20. Tewari KS, Monk BJ, Vergote I, et al. Survival with Cemiplimab in Recurrent Cervical Cancer. *N Engl J Med*. 2022;386(6):544–555.
21. Xu Q, Wang J, Sun Y, et al. Efficacy and Safety of Sintilimab Plus Anlotinib for PD-L1-Positive Recurrent or Metastatic Cervical Cancer: a Multicenter, Single-Arm, Prospective Phase II Trial. *J Clin Oncol*. 2022;40(16):1795–1805.
22. Melcher A, Harrington K, Vile R. Oncolytic virotherapy as immunotherapy. *Science*. 2021;374(6573):1325–1326.
23. Kim TK, Vandsemb EN, Herbst RS, Chen L. Adaptive immune resistance at the tumour site: mechanisms and therapeutic opportunities. *Nature Rev Drug Discovery*. 2022;21(7):529–540.
24. Huang X, He M, Peng H, et al. Genomic profiling of advanced cervical cancer to predict response to programmed death-1 inhibitor combination therapy: a secondary analysis of the CLAP trial. *J Immunother Cancer*. 2021;9(5).
25. Tamura K, Hasegawa K, Katsumata N, et al. Efficacy and safety of nivolumab in Japanese patients with uterine cervical cancer, uterine corpus cancer, or soft tissue sarcoma: multicenter, open-label Phase 2 trial. *Cancer Sci*. 2019;110(9):2894–2904.
26. Jardim DL, Goodman A, de Melo Gagliato D, Kurzrock R. The Challenges of Tumor Mutational Burden as an Immunotherapy Biomarker. *Cancer Cell*. 2021;39(2):154–173.
27. Le DT, Durham JN, Smith KN, et al. Mismatch repair deficiency predicts response of solid tumors to PD-1 blockade. *Science*. 2017;357:6349):409–413.
28. Zhang L, Luo M, Yang H, Zhu S, Cheng X, Qing C. Next-generation sequencing-based genomic profiling analysis reveals novel mutations for clinical diagnosis in Chinese primary epithelial ovarian cancer patients. *J Ovarian Res*. 2019;12(1):19.

29. Zou R, Xu H, Li F, Wang S, Zhu L. Increased Expression of UBE2T Predicting Poor Survival of Epithelial Ovarian Cancer: based on Comprehensive Analysis of UBE2s, Clinical Samples, and the GEO Database. *DNA Cell Biol*. 2021;40(1):36–60.
30. Liu C, Zhang Y, Hang C. Identification of molecular subtypes premised on the characteristics of immune infiltration of endometrial cancer. *Ann Translational Med*. 2022;10(6):337.
31. Park E, Kim SW, Kim S, et al. Genetic characteristics of gastric-type mucinous carcinoma of the uterine cervix. *Mod Pathol*. 2021;34(3):637–646.
32. Prieske K, Alawi M, Oliveira-Ferrer L, et al. Genomic characterization of vulvar squamous cell carcinoma. *Gynecol Oncol*. 2020;158(3):547–554.
33. Liu J, Li Z, Lu T, et al. Genomic landscape, immune characteristics and prognostic mutation signature of cervical cancer in China. *BMC Med Genomics*. 2022;15(1):231.
34. Saito Y, Takasawa A, Takasawa K, et al. Aldolase A promotes epithelial-mesenchymal transition to increase malignant potentials of cervical adenocarcinoma. *Cancer Sci*. 2020;111(8):3071–3081.
35. Tian W, Zhou J, Chen M, et al. Bioinformatics analysis of the role of aldolase A in tumor prognosis and immunity. *Sci Rep*. 2022;12(1):11632.
36. Wei X, Sha Y, Wei Z, et al. Bi-allelic mutations in DNAH7 cause asthenozoospermia by impairing the integrality of axoneme structure. *Acta Biochim Biophys Sin (Shanghai)*. 2021;53(10):1300–1309.
37. Gao Y, Liu L, Shen Q, et al. Loss of function mutation in DNAH7 induces male infertility associated with abnormalities of the sperm flagella and mitochondria in human. *Clin Genet*. 2022;102(2):130–135.
38. Van Duzer A, Taniguchi S, Elhance A, Tsujikawa T, Oshimori N. ADAP1 promotes invasive squamous cell carcinoma progression and predicts patient survival. *Life Science Alliance*. 2019;2(6):67.
39. Liu H, Zhao H. Prognosis related miRNAs, DNA methylation, and epigenetic interactions in lung adenocarcinoma. *Neoplasma*. 2019;66 (3):487–493.
40. van der Lely L, Häfliger J, Montalban-Arques A, et al. Loss of PTPN23 Promotes Proliferation and Epithelial-to-Mesenchymal Transition in Human Intestinal Cancer Cells. *Inflammatory Intestinal Dis*. 2019;4(4):161–173.
41. Jariwala N, Mendoza RG, Garcia D, et al. Posttranscriptional Inhibition of Protein Tyrosine Phosphatase Nonreceptor Type 23 by Staphylococcal Nuclease and Tudor Domain Containing 1: implications for Hepatocellular Carcinoma. *Hepatology commun*. 2019;3(9):1258–1270.
42. Yamada Y, Miyamoto T, Higuchi S, et al. cDNA expression library screening revealed novel functional genes involved in clear cell carcinogenesis of the ovary in vitro. *J Obstet Gynaecol*. 2021;41(1):100–105.
43. Springwald A, Lattrich C, Skrzypczak M, Goerse R, Ortmann O, Treeck O. Icb-1 Gene expression is elevated in human endometrial adenocarcinoma and is closely associated with HER2 expression. *Cancer Invest*. 2010;28(9):904–909.
44. Holohan C, Van Schaeybroeck S, Longley DB, Johnston PG. Cancer drug resistance: an evolving paradigm. *Nat Rev Cancer*. 2013;13(10):714–726.
45. Marusyk A, Almendro V, Polyak K. Intra-tumour heterogeneity: a looking glass for cancer? *Nat Rev Cancer*. 2012;12(5):323–334.
46. de Bruin EC, Taylor TB, Swanton C. Intra-tumor heterogeneity: lessons from microbial evolution and clinical implications. *Genome Med*. 2013;5 (11):101.
47. Burrell RA, McGranahan N, Bartek J, Swanton C. The causes and consequences of genetic heterogeneity in cancer evolution. *Nature*. 2013;501 (7467):338–345.
48. Pfeifer GP. Mutagenesis at methylated CpG sequences. *Curr Top Microbiol Immunol*. 2006;301:259–281.
49. Huang X, He M, Peng H, et al. Integrated genomic and molecular characterization of cervical cancer. *Nature*. 2017;543(7645):378–384.
50. Gagliardi A, Porter VL, Zong Z, et al. Analysis of Ugandan cervical carcinomas identifies human papillomavirus clade-specific epigenome and transcriptome landscapes. *Nat Genet*. 2020;52(8):800–810.
51. Christensen S, Van der Roest B, Besselink N, et al. 5-Fluorouracil treatment induces characteristic T>G mutations in human cancer. *Nat Commun*. 2019;10(1):4571.